



UNIVERSITY OF OKLAHOMA

GRADUATE COLLEGE

SIMPLE MODIFICATION METHOD FOR THE SURFACE FUNCTIONALIZATION  
OF POLY ( $\alpha$ -HYDROXY ESTER) POLYMERS

A THESIS

SUBMITTED TO THE GRADUATE FACULTY

in partial fulfillment of the requirements for the

Degree of

MASTER OF SCIENCE

By


JIMMY DAVID MURRAY  
Norman, Oklahoma  
2012

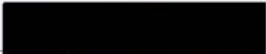
THESES  
MUR  
Cop. 2


SIMPLE MODIFICATION METHOD FOR THE SURFACE FUNCTIONALIZATION  
OF POLY ( $\alpha$ -HYDROXY ESTER) POLYMERS

A THESIS APPROVED FOR THE  
DEPARTMENT OF BIOENGINEERING

BY


  
Dr. Vassilios Sikavitsas, Chair

  
Dr. Edgar O'Rear

  
Dr. Robert Shambaugh

THE MOTHER OF ALL THINGS BEING CALLED, FOR ALWAYS ENCOURAGING  
TO BE OPEN, TO BE MOVING, TO BE HAPPY, AND MY SON, WHAT  
A BEAUTIFUL AND BEAUTIFUL SON AGAINST ALL

THIS IS DEDICATED TO MY WIFE, DANIELLE, FOR ALWAYS ENCOURAGING ME AND GIVING UP SO MUCH FOR THIS TO HAPPEN, AND MY SON, WYATT FOR BRINGING ME SO MUCH JOY AND INSPIRATION.



## Acknowledgements

There are so many people that I would like to acknowledge for helping me. First, I would like to thank my family. Without my mother and father, their encouragement, and unrelenting support I would not be here today. Even though I haven't always believed in myself they have always been there for me, giving all that they could to help me. They have been an inspiration for me, show me workmanship, honor, and loyalty and giving me a model for what I should be. My brothers and sister have challenged me, and set a standard that has pushed me to be better and smarter. You are all such great people, have such great families, and are amazing family members. You have challenged me relentlessly, showed me kindness with I didn't deserve it, and been there for me when I needed it most. Thank you all for everything.


Second, I would like to acknowledge all those whom I have worked with through my time here at the University of Oklahoma. I have always found that you are more than willing to give advice and some of your time for questions that I might have. This atmosphere has allowed me to grow and become more confident in myself. Of course it has also been very helpful when I have been confounded by a particular part of this project. I owe you all a lot and hopefully have shown you some of the helpfulness you have shown me.

Finally, I would like to acknowledge my wife, the rock of my life and my Evenstar. You showed me strength in me I couldn't find, love when I needed it most, and encouragement to get me through the toughest of times. To my son, Wyatt, and my children still to come, I love you all and strive to be my best so that you may be yours.




## Table of Contents

Acknowledgements.....	iv
Table of Contents.....	v
Table of Figures and Tables.....	vii
Table of Abbreviations .....	x
1.0 Abstract.....	xii
1.1 Introduction.....	1
1.2 Materials .....	5
1.3 Methods.....	6
1.3.1 Preparation of 2-D films .....	6
1.3.2 Entrapment of PolyK in PLA films .....	6
1.3.3 Verification of uniform entrapment.....	7
1.3.4 Stability of entrapment in PLA.....	7
1.3.5 Linking a biological molecule to polyK .....	8
1.3.6 Linking of fluorescent HE to films and fibers .....	9
1.3.7 Collection of rat mesenchymal stem cells .....	9
1.3.8 Cell attachment to scaffolds.....	9
1.3.9 Scaffold cellularity.....	10
1.3.10 PolyK cytotoxicity .....	11
1.3.11 PolyK entrapment in polymer films.....	12




1.3.12 Statistical analysis.....	13
1.4 Results.....	13
1.4.1 Entrapment of polyK in 2-D films.....	13
1.4.2 Verification of uniform entrapment.....	16
1.4.3 Optimal process time and stability of entrapment of polyK in PLA .....	17
1.4.4 Linking of fluorescent HE to films and fibers .....	19
1.4.5 Scaffold Cellularity.....	21
1.4.6 PolyK Cytotoxicity .....	24
1.4.7 PolyK Entrapment in Polymer Films.....	25
1.5 Discussion .....	28
1.6 Conclusion .....	38
1.7 References.....	40



## Table of Figures and Tables

- Figure 1** Two methods were used to entrap PA into a polymer network of PLA. Method (1) uses acetone/water to swell the polymer network, and then a solution of 0.1 mg/mL PA in DMSO to entrap. Method (2) used a single solution of 0.1 mg/mL PA in acetone/water to entrap. .... 14
- Figure 2** The standard curve of absorbance of an ABTS sample vs. molar HRP  $\times 10^{12}$  adsorbed to PLA surface. Linear regression was used to obtain a linear fit within a 95% confidence interval (not shown). .... 14
- Figure 3** Quantification of PA entrapped using two different entrapment techniques. Techniques include polyK and PEG-amine using method (1), acetone/water soaking and then incubation in DMSO with a PA concentration of 0.1 mg/mL, and method (2), acetone/water soaking with a PA concentration of 0.1 mg/mL. Adsorbed p-HRP was subtracted out to give the values shown. (n=4, \* p<0.001) ..... 15
- Figure 4** Fluorescent micrographs, using an exposure time 100 ms, of the surface of PLA modified with polyK (A) and not modified with polyK (B). Both films were treated with NHS-rhodamine. The scale bar is 1000  $\mu\text{m}$ ..... 16
- Figure 5** A schematic of the movement of PA into the polymer network during entrapment and then the diffusion of the PA out of the scaffold after a period of time. .. 17
- Figure 6** Quantified entrapment of polyK with increasing time including 12, 24, and 48 hours. Each group was washed for a given period in PBS at pH = 7.3, and then assayed using p-HRP and ABTS. The control group of HRP adsorbed on the surface was subtracted from the total to give the values shown. (n=4, \* = p<0.001, # p > 0.05 [compared to control]) ..... 18





**Figure 7** Fluorescent micrographs, using an exposure time of 4000 ms, of the surface of PLA modified with the PA, polyK, linked to HE-FITC (left) and only incubated with HE-FITC showing HE physisorption (right). Both films were treated with heparin modified with EDC and NHS. The scale bar is 395  $\mu\text{m}$ ..... 20

**Figure 8** PLA fiber scaffolds were modified with the PA, polyK, and linked to HE-FITC (A), only modified with the PA polyK (B), and only incubated with HE-FITC showing HE physisorption (C). The scale bar is 395  $\mu\text{m}$ . ..... 20

**Figure 9** Fluorescent micrographs, using an exposure time of 4000 ms, of statically seeded rMSCs showing the cellular shape taken on the surface of PLA modified with (A) nothing (B) polyK (C) HE (D) HA. Cellular F-actin filaments were stained using phalloidin. Scaffolds modified with HE or HA show cell stretching, while scaffolds with no modifications, or only polyK show limited stretching on the fiber surface. HE modified scaffolds show stretched cells along PLA fibers and across fibers. HA modified scaffolds show less stretched cells than heparin modified scaffolds, but more stretching than polyK modified scaffolds..... 22

**Figure 10** Picogreen DNA assay results showing the scaffold cellularity with covalently linked to biological molecules, plain bars, versus scaffolds with adsorbed molecules and plain scaffolds, bars crosshatched. HE and HA were linked to the scaffold using a zero length carbodiimide linker and RGDC was linked using 6.8 Å spacer arm linker. Cell number was found from a picogreen DNA assay using the assumption of 7 pg/cell. (n =4, \* p<0.05 compared to control, # p>0.05 compared to the plain scaffold) .. 23


**Figure 11** The results are shown for the alamar blue assay for modified group, fiber scaffolds with polyK entrapped, and the control, no polyK entrapped. The results

show negligible difference between the modified group and the control. Fluorescence was measured using an opaque white 96 – well plate and 300  $\mu$ L of each sample. The samples were measured at 530 nm excitation and 590 nm emission. (n = 3, p>0.05) ..... 25

**Figure 12** The qualitative amount of different polymer anchors entrapped in PCL, PLA, PLGA (85:15), and PLGA (50:50). The amount of both entrapped polyK and percent amorphous increase from left to right. For each polymer, the amount of HRP covalently linked to a polyK was statistically higher than PEG-amine or RL-peptide. The amount of polyK also entrapped in PLGA85 and PLGA50 was statistically higher than PCL and PLA. (n=4, \* p<0.05, # highest absorbance, & p>0.05)..... 26

**Figure 13** The quantitative measurement of the amount of polyK entrapped into different poly ( $\alpha$ -hydroxy esters). There is an increase in the amount of the polyK entrapped in the highly amorphous structure of PLGA50 and PLGA85 (indicated by &), while the more crystalline structure of PLA and PCL showed lower entrapped polyK per  $\text{cm}^2$ . The highest amount of entrapped polyK is shown by \*. (n = 4, \$ p > 0.05) ..... 27

**Table 1** Representative crystallinity values for poly ( $\alpha$  – hydroxy ester) polymers used in this study..... 37



## Table of Abbreviations

ABTS = 2, 2'-Azinobis [3-ethylbenzothiazoline-6-sulfonic acid]-diammonium salt

$\alpha$  - MEM = GIBCO Minimum Essential Media Alpha Medium

EDC= 1-Ethyl-3-[3-dimethylaminopropyl] carbodiimide hydrochloride

ECM = Extracellular matrix

FGF = fibroblast growth factor

HA= Hyaluronic acid sodium salt from Streptococcus equi

HE= Heparin sodium salt from bovine intestinal mucosa

HE-FITC= Heparin with fluoresceine isothiocyanate

HEPES = N-2-Hydroxyethylpiperazine-N'-2-ethanesulfonic acid, free acid

MES= 2-(N-morpholino) ethanesulfonic acid, monohydrate

MSC = Mesenchymal stem cell

NHS= N-hydroxysuccinimide


NHS-rhodamine = 5/6-carboxy-tetramethyl-rhodamine succinimidyl ester


PA= Polymer anchors

PBS= Phosphate buffered saline

PCL= poly ( $\epsilon$ -caprolactone)

PEG = poly (ethylene glycol)





PEG-amine = Homobifunctional poly (ethylene glycol) with amine functional end groups

p-HRP= EZ-Link Plus Activated Peroxidase

PGA = polyglycolic acid

PLLA = Poly (L-lactic acid)

PLA = 1.49% D poly (D, L-lactic acid)

PLGA85= poly (D, L – lactide – co glycolide) (85:15)

PLGA50= poly (D, L – lactide – co – glycolide) (50:50)

PolyK = poly -ε - CBZ – L-lysine

RGD= arginine – glycine – aspartic acid peptide

RGDC= arginine – glycine – aspartic acid – cysteine peptide

RL-peptide = Arginine – Leucine di-block peptide (RRRRRRRLLLLLLK)


rMSC= rat mesenchymal stem cell

SPDP = Succinimidyl 3-(2-pyridyldithiol) propionate

TE = Tissue Engineering

TFE = 2, 2, 2 - trifluoroethanol

VEGF = vascular endothelium growth factor



## 1.0 Abstract


A vital component for the engineering of tissue constructs *in vitro* is a scaffold that allows cells to adhere and proliferate. Biomimetic scaffolds aim to enhance the regeneration of damaged tissue by mimicking the cells' natural environment. This study investigated the potential of surface functionalization of PLA films. PLA fibers were modified using an acetone-water mixture to physically entrap amine functionalized polyK uniformly. Biomimetic modification was achieved with linking of biological molecules using amine coupling chemistry (amine to carboxylic acid using a carbodiimide). Uniform surface coverage of entrapped and linking molecules was shown using fluorescent microscopy. Process flexibility is demonstrated with cellular response to surface modification using HE, HA, and RGD. Initial cell response was investigated with a statically attached cell culture of rMSC's, F-actin staining, and fluorescent microscopy. This imaging showed surface modification enhanced cell attachment, cell stretching, and can potentially signal cell differentiation. Expansion of the process to more materials showed a preference for amorphous structure over crystallinity in poly ( $\alpha$ -hydroxy esters). This process is a simple method for uniform surface modification that is non-destructive to the scaffold and can be used to attach many biological molecules (proteins, peptides, and GAG's) in order to present a cell friendly surface.



## 1.1 Introduction

Tissue engineering applies biological and engineering principles toward the development of tissue and organ substitutes [1]. In general, cells are extracted from a patient or donor, given chemical and mechanical stimulation during culture via a scaffold and a bioreactor, and transplanted into the patient for tissue restoration and improvement. Stem cells, such as MSC's, are widely used because of the potential to create multiple tissues from one cell source [2]. It has been found that MSC's can be harvested from multiple adult tissues and differentiated into several cell types such as neurons, chondrocytes, osteoblasts, and cardiomyocytes [3-5]. These processes have been used to regenerate skin [6, 7], bone[8, 9], cartilage[10, 11], nerves[12, 13], and heart valves[14, 15].

The cell environment is one of the keys to control the final differentiation of the stem cell [16, 17]. This interaction between the cell and scaffold is important to tissue engineers [18, 19]. Early biomaterials primarily provided structural support for tissue reconstruction. The next generation of biomaterials focused on producing bioactive materials. Today, third generation biomaterials provide mechanical support, mimic the physiological environment, and direct tissue formation and reconstruction at the cellular level [20]. Polymers, both synthetic and natural, have been used. Natural polymers provide benefits such as inherent biological recognition molecules, cell receptor binding domains, but synthetic materials allow for more control of material properties [16]. Synthetic materials used as biomaterials should evoke a limited sustained inflammatory response, degrade in proportion to tissue formation, have mechanical properties appropriate for intended use, and produce non-toxic degradation by-products [21]. In

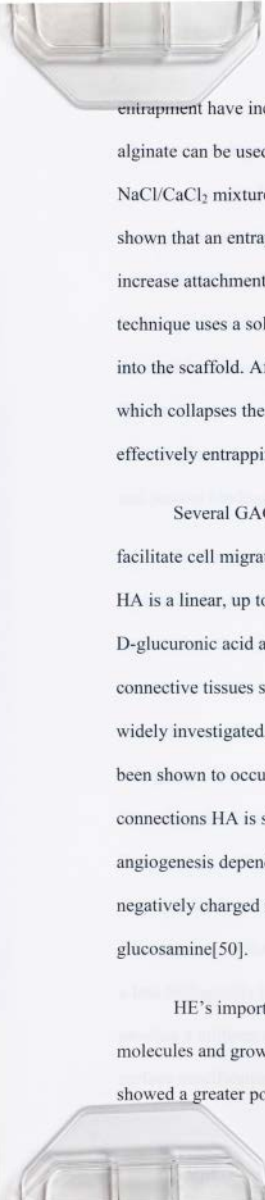


addition, three dimensional biomaterials or tissue engineering scaffolds should provide support for cell proliferation, migration, and nutrient transport via systems of interconnected pores[22].

Poly ( $\alpha$ -hydroxy esters) are biodegradable polymers widely used as tissue engineering scaffolds particularly, PLLA, PGA, and their copolymers. These polymers have been used to create scaffolds with multiple architectures but as plain biomaterials, scaffolds without modifications such as plasma treatment, chemical treatment, or any molecules linked covalently or by physisorption, shows limited ability for cell adhesion and growth and cannot direct cell differentiation or mimic the physiological environment [23]. In order to achieve these goals, the scaffold is modified to create a biomimetic scaffold. This is done by modifying the scaffold surface with biological molecules such as growth factors or ECM molecules to mimic the ECM during repair. Modification is performed either as bulk modification or surface modification [24, 25]. Several techniques are used to impart biological molecules including physisorption [26, 27], chemical crosslinking of the polymer scaffold [28, 29], and covalent attachment to the surface[30, 31]. The latter technique can be done provided a functional group is available on the scaffold surface. In order to provide this functional group the surface can be activated via plasma treatment[32], hydrolysis[33], aminolysis[34], or by physical entrapment of a functionalized polymer anchor.

Physical entrapment was first introduced by Hubbell et al. to show that PEG could be entrapped in a polymer surface using a solvent/non-solvent technique [35, 36]. This technique was expanded on by Quirk et al. to successfully entrap poly (L-lysine) on PLLA and was shown to effect cell attachment [37, 38]. While most instances of physical






entrapment have included a hydrophobic polymer network, Hou et al. showed that alginate can be used to physically entrap PEG and poly (L-lysine). This procedure used a NaCl/CaCl<sub>2</sub> mixture followed by a CaCl<sub>2</sub> to entrap the PA [39]. Recently, our group has shown that an entrapped PA can be further linked to adhesive molecules such as RGD to increase attachment and direct MSC differentiation to osteoblasts [40-42]. In general this technique uses a solvent to swell the polymer scaffold, which allows the PA to diffuse into the scaffold. After a short period of time, the scaffold is then soaked in a non-solvent which collapses the scaffold (returning the polymer network to its original state), effectively entrapping the PA at the surface of the scaffold.

Several GAGs found in the extracellular matrix can enable cell attachment, facilitate cell migration, store and release growth factors, and trigger MSC differentiation. HA is a linear, up to 10<sup>7</sup> Dalton, non-sulfated GAG, composed of alternating (1→4) – β-D-glucuronic acid and (1→3) – β-N-acetyl-D-glucosamine, found in the ECM of connective tissues such as bone or cartilage [43, 44]. HA as a natural TE scaffold has been widely investigated, but it can also be used as a signaling molecule. Cell-HA binding has been shown to occur via the CD44 and RHAMM receptors [45, 46]. Through these connections HA is shown to trigger increased cell motility, angiogenesis, and even anti-angiogenesis depending on molecular weight [47-49]. HE is a highly sulfated, highly negatively charged GAG composed of α or β (1-4) linked uronic acid and α-D-glucosamine [50].


HE's importance comes from its ability to interact with several key ECM molecules and growth factors. Singh et al. recently reported that VEGF captured by HE showed a greater potential for angiogenesis than VEGF covalently linked to PEG [51].






The interactions are not limited to VEGF, but also include FGF, fibronectin, and vitronectin. Sakiyama-Elbert et al. used HE for the controlled release of growth factors for nerve growth. This process showed an increase in neurite extension of 100% compared to non-heparinized materials [52]. Another study used an alginate hydrogel with linked HE to bind bone morphogenic protein – 2 (BMP-2) and controllably release it. This process showed 1.9 fold increase in peripheral bone formation and 1.3 fold increase in calcium deposition compared to alginate scaffolds without HE [53]. Therefore HE can be used to create a better biomimetic scaffold by utilizing its multiple properties of cell adhesion and growth factor release. A complete discussion of HE growth factor and protein binding has been provided by Capila et al[54].

In this study a simple surface modification technique was introduced in order to present amine functional groups for biological modification. This functionality provides a surface that, through amine coupling chemistry, can be made biologically active. With the current variety of linkers available virtually any biological molecule can be linked to the surface to elicit a specific cellular response. In a previous study by this lab a PA with side groups was used that is thought to have detrimental long term effects *in vivo*. Therefore, the first goal of this study was to replace the PA previously used by Alvarez – Barreto et al. with PEG-amine, based on PEG, a widely used polymer, which has been shown to limit cell attachment and immune response *in vivo*. The second goal was to eliminate one of the solvents (DMSO) used during entrapment by only using one step and a less biologically harsh solvent, an acetone/water solution, to entrap a PA and still produce a uniform and stably modified surface. The third goal was to improve upon the surface modification previously shown, linking small polypeptides (RGD), by covalently





linking large molecules, HA or HE, to the surface. The final goal was to show the versatility of the process by entrapping a PA in different poly ( $\alpha$  - hydroxy ester) polymers.

## 1.2 Materials

PLA (MW = 108500) was provided by Nature Works LLC. PCL ( $M_w$  = 117600 ,  $M_n$  = 63600), PLGA85 ( $M_w$  = 89300,  $M_n$  = 49100), and PLGA50 ( $M_w$  = 122000,  $M_n$  = 71000) were provided by Durect Corp.( Birmingham, AL). Poly- $\epsilon$ -CBZ-L-lysine (MW = 1000 – 4000), Heparin sodium salt from bovine intestinal mucosa(180 USP units/mg), Hyaluronic acid sodium salt from Streptococcus equi (MW = 1,630,000) was purchased from Sigma-Aldrich (St. Louis, MO). OmniPur® MES, monohydrate and OmniPur® HEPES, free acid were purchased from EMD Millipore (Billerica, MA). Heparin-FITC (MW = 3000-30000) was purchased from Polysciences, Inc. (Warrington, PA). EDC, NHS, NHS-rhodamine, SPDP, and p-HRP were purchased from Pierce Biotechnology (Rockford, IL). ABTS, GIBCO Minimum Essential Media Alpha Medium, and Alexa Fluor 488 phalloidin were purchased from Invitrogen (Camarillo , CA). Triton X-100 and 10% Formalin in phosphate buffered saline was purchased from VWR (Suwanee, GA). Chloroform and acetone were purchased from Fisher Scientific (Pittsburgh, PA). PEG-amine (MW = 20,000) with terminal amine functional groups was purchased from Laysan Bio, Inc. (Arab, AL).



## **1.3 Methods**

### **1.3.1 Preparation of 2-D films**

PLA films were prepared by dissolving PLA in chloroform at a concentration of 50 mg/mL. The mixture was poured evenly in 60 mm petri dishes to dry overnight. The dried films were then extracted from the petri dishes and stored under vacuum until use.


### **1.3.2 Entrapment of PolyK in PLA films**

PLA films were cut to a standard size of 8 mm in diameter and  $140 \pm 6.3 \mu\text{m}$  in thickness. The optimal procedure to entrap was found by testing 2 different groups as follows:

1. PLA films were soaked in 600  $\mu\text{L}$  of a 70/30 acetone/water (v/v) mixture for 1 hour and then incubated in 0.1 mg/mL polyK or PEG-amine dissolved in 2.5 mL DMSO for 12 hours.

2. PLA films were incubated in 2.5 mL of 70/30 acetone/water (v/v) mixture with 0.1 mg/mL dissolved polyK or PEG-amine for 12 hours.

The entrapment technique was evaluated by incubating modified films in p-HRP at  $10^{-8}$  M in PBS (pH = 7.3) for 2 hours. After a wash in 1% Triton X-100 and three washes of deionized (DI) water, films were incubated in ABTS single solution, solution provided previously prepared by the manufacturer at unknown concentration (Invitrogen, Camarillo, CA) for 30 minutes. HRP catalyzes the reaction of ABTS and peroxide P-HRP activity was measured by reading absorbance in a Synergy HT plate reader (Bio-Tek, Winooski, VT) at 415 nm. Levels of polyK entrapment were quantitatively related to the absorbance signal by a standard curve prepared as follows.



Films were punched as previously specified and 20  $\mu$ L of p-HRP solution was pipetted on the surface. This was allowed to incubate for 30 minutes to let physisorption occur. Next, the prepared films were incubated in ABTS single solution for 30 minutes and then assayed in triplicate. P-HRP activity was measured by reading absorbance in a Synergy HT plate reader (Bio-Tek, Winooski, VT) at 415 nm. A control of a film with no HRP in ABTS and ABTS with no film was used. This curve allowed for quantification of the PA entrapped from 300 to 0.03 picomolar. This standard was used throughout this investigation to quantify the amount of PA entrapped to the surface.

### **1.3.3 Verification of uniform entrapment**

After modification, scaffolds were incubated in 0.4 mM NHS-rhodamine in PBS at pH=7.2 for 30 minutes, and then washed once with 1% Triton X-100 and three times with DI water. Fluorescence microscopy of modified and unmodified discs was performed using a Nikon Epifluorescence microscope (Lewisville, TX) with excitation at 552 nm and emission at 575 nm. Images were captured with MetaMorph 6.2 (Universal Imaging Corporation, Downingtown, PA). (n=4)

### **1.3.4 Stability of entrapment in PLA**

The optimal time for entrapment and the stability of entrapped polyK in PLA was tested. Films were incubated for 12, 24, and 48 hours using procedure 2 with 0.1 mg/ml polyK, and then incubated in PBS for 8 days. At day 0 and then every two days, films were modified further with p-HRP for use in an absorbance assay. Films were incubated in p-HRP in PBS for 2 hours and then washed in 600  $\mu$ L of 1% Triton X-100 once and DI water three times. Films were incubated in ABTS single solution for 30 minutes to monitor HRP activity. Activity was measured by reading absorbance in a Synergy HT




plate reader (Bio-Tek, Winooski, VT) at 415 nm. Levels of polyK entrapment were quantitatively related to absorbance using the standard curve described in section 1.3.2.

(n=4)

### **1.3.5 Linking a biological molecule to polyK**

Biological modification of entrapped polyK in fiber scaffolds was performed for both HE and HA using the following technique (GAG will signify HE or HA). The carboxyl group of the GAG was activated by addition of EDC and NHS. EDC at 2 mM and NHS at 5 mM were reacted with 0.01 mg/mL HE or HA in MES buffer at pH 6 for 15 minutes. NHS was added to stabilize the EDC/GAG conjugate to link with the amine group of polyK. Next, an equal volume of PBS was added to increase the solution pH to 7.1. Films were then added to 600  $\mu$ L of this solution and fibers were added to 1 mL of this solution and reacted for 2 hours. Each scaffold was then washed, fibers with 1 mL and films with 600  $\mu$ L.

To test the improvement of cell adhesion of the HE and HA, RGD was also linked to polyK using a previously described method[40]. First, 0.4 mM SPDP was dissolved in DMSO and diluted to 0.1 mM in PBS at pH = 7.4, and then reacted with modified films or fibers for 30 minutes. Each scaffold was then washed as described above and reacted with 0.1 mM RGDC in HEPES at pH = 8.3 for 90 minutes at 40 °C[55]. After further washing the scaffolds were placed in PBS until use. Sterile procedures were carefully followed when modified films or fibers were cultured with cells following modification.



### **1.3.6 Linking of fluorescent HE to films and fibers**

Films and fibers were modified with HE-FITC as described in the previous section. Each film or fiber was then washed as previously described, fibers with 1 mL and films with 600  $\mu$ L in a dark box. Fiber scaffolds were isolated and mechanically opened. Single fibers were taken from the center to test modification throughout the scaffolds. Fluorescence microscopy of modified and unmodified films and fibers was performed using a Nikon Epifluorescence microscope (Lewisville, TX) with excitation at 419 nm and emission at 516 nm. Images were captured with MetaMorph 6.2 (Universal Imaging Corporation, Downingtown, PA). (n=4)


### **1.3.7 Collection of rat mesenchymal stem cells**

Adult rMSC were isolated from the bone marrow of 8-week-old male Wistar rats (Harlan Laboratories, Indianapolis, IN) using well-established methods. Briefly, rats were euthanized, and the tibiae and femora were extracted. The epiphyses were cut off, and the bone marrow was flushed and suspended in  $\alpha$ -MEM supplemented with 10% fetal bovine serum. The suspension was then distributed in polystyrene culture flasks (75 cm<sup>2</sup>). Cells were cultured at 37 °C and 5% carbon dioxide. Non-adherent cells were discarded after 2 days of culture. MSCs were detached using trypsin, centrifuged at 400 g for 5 min, resuspended in  $\alpha$ -MEM, and replated until the third passage.

### **1.3.8 Cell attachment to scaffolds**

A static culture of third passage rMSC's was used to assess the effect of the modification on cell attachment. Third passage rMSC's were used at a density of 800,000 cells/mL and 200,000 cells/scaffold for fiber scaffolds in  $\alpha$ -MEM. Fiber scaffolds were pre-wet with 95% ethanol under vacuum to remove air bubbles. Scaffolds were washed in






PBS for 1 hour, fitted into cassettes for static culture, and then the specified cell concentration was added and incubated for 6 hours.

After incubation, the scaffolds were washed with PBS and then soaked in 10% Formalin in PBS at 4 °C overnight. Next, scaffolds were allowed to equilibrate to room temperature for 30 minutes. Alexa Fluor 488 phalloidin was used to stain the F-actin filaments of cells attached to fiber scaffolds at the concentration specified by the manufacturer. Alexa Fluor 488 phalloidin was dissolved in methanol at 6.6  $\mu\text{M}$ , and then diluted into PBS to 1.65  $\mu\text{M}$ . Scaffolds were first rinsed in 0.1% Triton X-100 and PBS at a pH of 7.3. Next, 200  $\mu\text{L}$  of the phalloidin solution was pipetted onto the scaffolds and allowed to incubate for 30 minutes. Fluorescence microscopy of modified and unmodified fiber scaffolds was performed using a Nikon Epifluorescence microscope (Lewisville, TX) with excitation at 495 nm and emission at 518 nm. Images were captured with MetaMorph 6.2 (Universal Imaging Corporation, Downingtown, PA).

### **1.3.9 Scaffold cellularity**

A static culture of third passage rMSC's was used to assess the effect of the modification on scaffold cellularity. Third passage rMSC's were used at a density of 2,000,000 cells/mL and 500,000 cells/scaffold for fiber scaffolds in  $\alpha$ -MEM. Fiber scaffolds were pre-wet with 95% ethanol under vacuum to remove air bubbles. Next, scaffolds were washed in PBS for 1 hour, fitted into cassettes for static culture, and then the specified cell concentration was added and allowed to incubate for 6 hours. After incubation, scaffolds were rinsed in PBS and suspended in 3 mL nanopure water. Three freeze thaw sessions were performed to lyse the cells. A picogreen DNA quantification assay was then performed to assess scaffold cellularity.




A standard curve was generated from known concentrations of  $\lambda$ DNA. Samples and standards were prepared using aliquots of 43  $\mu$ L in a 96 well plate. Next 107  $\mu$ L of reaction buffer ( $20 \times 10^{-3}$  M Tris-HCl,  $1 \times 10^{-3}$  M EDTA, pH=7.5) was added to each well. Picogreen dye was added to bring the total volume to 300  $\mu$ L. Fluorescence was measured using a Synergy HT plate reader (Biotek) at 490 nm excitation and 520 nm emission. The number of cells was calculated using the total amount of DNA in a sample divided by the total amount of DNA in one cell, 7 pg [56].(n=4)

### 1.3.10 *PolyK cytotoxicity*

rMSC's were cultured on fiber scaffolds for 2 days in order to analyze the cytotoxicity of entrapped polyK. There were two groups investigated, groups with entrapped polyK and those without. rMSC's at the third passage were uniformly suspended and seeded statically onto fiber scaffolds. Cells were allowed to adhere for 8 hours, and incubated for 2 days at 37 °C and 5% CO<sub>2</sub>. Then an alamar blue assay was performed. Alamar blue was added, 10% of the total volume, and allow to incubate for 4 hours. Next, 300  $\mu$ L were aliquoted to a 96-well plate and the fluorescence was measure using a Synergy HT plate reader (Bio-Tek, Winooski, VT) at excitation 530 nm and emission 590 nm. The cytotoxicity was calculated as the percent viable by dividing the fluorescence of a sample group by the fluorescence of the control group. (n=4)

The scaffolds were then washed with PBS and frozen in 1.5 mL of nanopure water. After three freeze – thaw sessions the amount of cells was quantified using a picogreen DNA assay as previously described. A standard curve was generated from known concentrations of  $\lambda$ DNA. Samples and standards were prepared using aliquots of 43  $\mu$ L in a 96 well plate. Next 107  $\mu$ L of reaction buffer ( $20 \times 10^{-3}$  M Tris-HCl,  $1 \times 10^{-3}$  M






EDTA, pH=7.5) was added to each well. Picogreen dye was added to bring the total volume to 300  $\mu$ L. Fluorescence was measured using a Synergy HT plate reader (Biotek) at 490 nm excitation and 520 nm emission. The number of cells was calculated using the total amount of DNA in a sample divided by the total amount of DNA in one cell. This number was then used along with the alamar blue assay results to acquire a normalized result and negate any variability in cell seeding. This was done by dividing the fluorescence by the number of cells, and obtaining fluorescence per cell or the qualitative amount of resazurin reduced per cell. (n=4)

### **1.3.11 PolyK entrapment in polymer films**

Polymer films were produced by the method previously described. Films were created using PCL, PLA, PLGA85, and PLGA50. First, 100 mg/mL polymer solutions were created by dissolving the polymers in chloroform. Next, the films were poured evenly over 60 mm petri dishes and the chloroform was allowed to evaporate. The films were stored in a vacuum chamber. Special care was taken with PLGA85 and PLGA50. For each, aluminum was placed in the petri dishes and the solutions were poured over them. After drying the films were then able to be taken out of the petri dishes and were placed in a vacuum chamber until use.

Three different polymer anchors were investigated. The first was hydrophobic, polyK, the second was hydrophilic, PEG – amine, and the third was a di – block peptide of arginine and leucine (RL- peptide). The three polymer anchors were investigated separately. Briefly, films were punched according to the previous protocol, 8 mm in diameter and approximately 200  $\mu$ m in thickness. These films were then soaked for 12 hours in a 70% acetone and 30% water solution with 0.1 mg/mL of the polymer anchor.



The films were then rinsed in 0.1% triton X-100 for 15 minutes, and DI water three times for 15 minutes each to wash off adsorbed polymer anchors. Next, the films were incubated for 2 hours in  $10^{-8}$  M p-HRP in PBS (pH= 7.3). After rinsing the films as described above, the films were soaked in ABTS for 30 minutes. Finally, 150  $\mu$ L of ABTS solution was pipetted into a 96 well plate at triplicate. P-HRP activity was measured by reading absorbance in a Synergy HT plate reader (Bio-Tek, Winooski, VT) at 415 nm. The level of PA entrapment was directly related to p-HRP activity using a standard curve.

### **1.3.12 Statistical analysis**

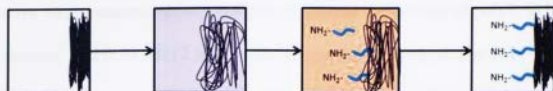
Statistical Analysis was performed using analysis of variance (ANOVA) with groups of  $n = 4$  unless otherwise stated. A Tukey test was then performed to analyze for significance between groups with a confidence level of 95%. Statistical significance was given for sample groups with  $p < 0.05$ . Values are reported as the means with error reported as standard error of the mean.

## **1.4 Results**

### **1.4.1 Entrapment of polyK in 2-D films**

Two different methods, shown in figure 1, were tested for entrapping PA into the surface of PLA. Method (1) uses an acetone/water solution and then DMSO with the PA. Method (2) uses only the acetone/water solution with the PA to entrap. To test the optimal method between (1) and (2), a colorimetric assay was performed using p-HRP and ABTS. Modification was then shown through a higher absorbance signal. This signal was used to create a standard curve, which was used to translate the absorbance signal to surface mole concentration ( $\text{femtomole}/\text{cm}^2$ ). The results are shown in figure 2.

Method (1)



Method (2)

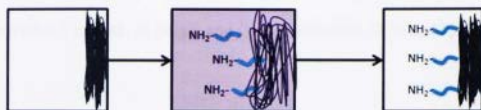


**Figure 1** Two methods were used to entrap PA into a polymer network of PLA. Method (1) uses acetone/water to swell the polymer network, and then a solution of 0.1 mg/mL PA in DMSO to entrap. Method (2) used a single solution of 0.1 mg/mL PA in acetone/water to entrap.

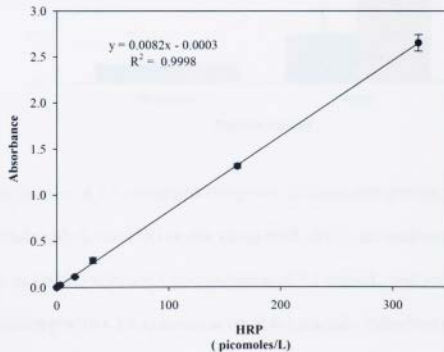


**Figure 2** The standard curve of absorbance of an ABTS sample vs. molar HRP  $\times 10^{12}$  adsorbed to PLA surface. Linear regression was used to obtain a linear fit within a 95% confidence interval (not shown).

Quantitative measurements, shown in figure 3, showed the amount of polyK to be  $0.99 \pm 0.15$  fmoles/cm<sup>2</sup> and  $0.20 \pm 0.12$  fmoles/cm<sup>2</sup> for method (2) and method (1) respectively. These results are not in agreement with previous reports where a variant of method (1) was used. Specifically, the previous method used an acetone/water wash then DMSO incubation with 0.1 mg/mL of polyK and PLLA films (0% D form of poly(L-lactic acid)) [40].

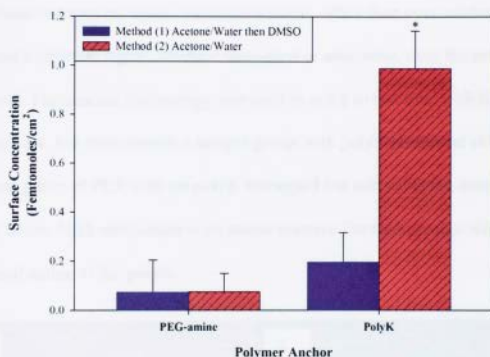


**Figure 3** Quantification of PA entrapped using two different entrapment techniques.

Techniques include polyK and PEG-amine using method (1), acetone/water soaking and then incubation in DMSO with a PA concentration of 0.1 mg/mL, and method (2), acetone/water soaking with a PA concentration of 0.1 mg/mL. Adsorbed p-HRP was subtracted out to give the values shown. (n=4, \* p<0.001)

The PA was then examined using polyK, a hydrophobic peptide, and PEG-amine, a hydrophilic polymer, and the results shown in figure 3. The amount of polyK entrapped was statistically higher than PEG-amine when using method (1) and method (2). Using

method (2) the amount of polyK was shown to be  $0.99 \pm 0.15$  fmoles/cm<sup>2</sup> or  $1.06 \pm 0.17$  pg, compared to  $0.08 \pm 0.07$  fmoles/cm<sup>2</sup> or  $0.08 \pm 0.08$  pg when using PEG-amine.

Therefore the polyK entrapped using method (2) showed the statistically highest amount of entrapped PA. For all further results, polyK was used with method (2) to entrap the PA.

#### 1.4.2 Verification of uniform entrapment

Uniform entrapment across the entire surface, rather than over random sections, would present a constant signal, whether biological or otherwise, over the entire surface of the material. Fluorescent microscopy was used in order to test this, with the results shown in figure 4. For these results a sample group with polyK entrapped at 0.1 mg/mL with a control group of PLA with no polyK entrapped but still using the acetone/water wash for 12 hours. NHS-rhodamine is an amine reactive fluorophore that will react with the N-terminal amine of the polyK.

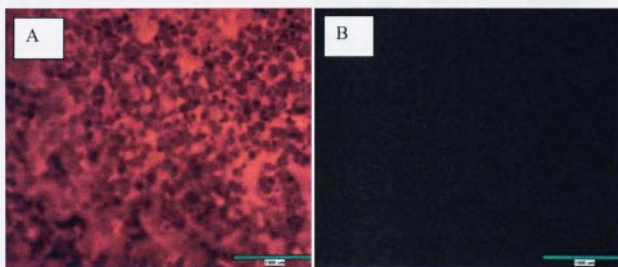


**Figure 4** Fluorescent micrographs, using an exposure time 100 ms, of the surface of PLA modified with polyK (A) and not modified with polyK (B). Both films were treated with NHS-rhodamine. The scale bar is 1000  $\mu$ m.

Therefore the entrapment as well as the spatial distribution was shown by the higher fluorescence of modified scaffolds than unmodified control scaffolds. Figure 4a shows a uniform red signal over the surface of the PLA film, while figure 4b shows a barely detected signal due to NHS-rhodamine physisorption. These results show that entrapment of polyK in this PLA surface presents a uniformly functionalized surface for further modification.

#### 1.4.3 Optimal process time and stability of entrapment of polyK in PLA

Physical entrapment involves the PA diffusing into a swollen polymer network. The time dependency of this diffusion was investigated. PLA films were exposed to equal amounts of polyK for the three different time periods of 12, 24, and 48 hours with results shown in figure 6. Control groups of plain PLA with physisorbed p-HRP were used. All groups showed higher polyK surface concentration at day 0, immediately following entrapment, than the control group. Comparing the initial surface concentration shows that the 24 hour time period was statistically higher than 12 hours with a surface concentrations of  $2.20 \pm 0.77$  fmoles/cm<sup>2</sup> and  $0.99 \pm 0.15$  fmoles/cm<sup>2</sup> respectively. The 48 hour time period initially entrapment concentration was not statistically different than either the 24 time period or the 12 hour time period with  $1.60 \pm 0.38$  fmoles/cm<sup>2</sup>.

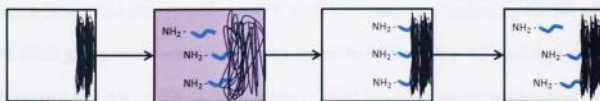



**Figure 5** A schematic of the movement of PA into the polymer network during entrapment and then the diffusion of the PA out of the scaffold after a period of time.

Stability of entrapment is an important factor for a biomaterial. Some applications need a constant signal while other applications prefer a varying signal. The surface is unstable if the PA diffuses out into solution from the polymer network. Samples were taken each two days for eight days with a control sample of adsorbed p-HRP on plain PLA films for each time period. There was a significant drop at day 6 for the entrapment time periods of 12 and 24 hours, while this drop occurred at day 4 for the 48 hour time period.

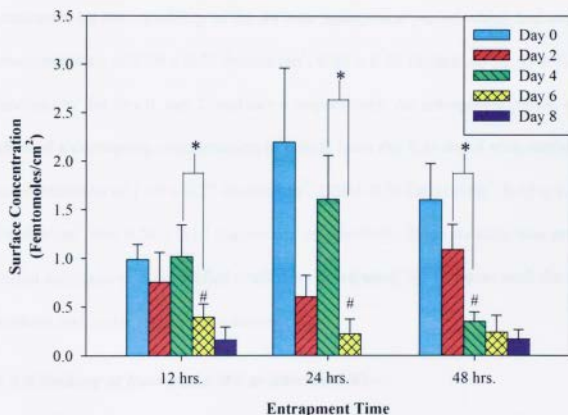


**Figure 6** Quantified entrapment of polyK with increasing time including 12, 24, and 48 hours. Each group was washed for a given period in PBS at pH = 7.3, and then assayed using p-HRP and ABTS. The control group of HRP adsorbed on the surface was subtracted from the total to give the values shown. (n=4, \* = p<0.001, # p > 0.05 [compared to control])





This drop shows entrapment for each time period is unstable. After the drop the next days were indistinguishable from the control group statistically. Therefore at those time periods, it is hypothesized all the polyK was diffused out of the network and into the solution.

The most stable entrapment method was shown to the 12 hour period, shown in figure 6, with a surface concentration of  $0.99 \pm 0.15$  fmoles/cm<sup>2</sup>,  $0.76 \pm 0.31$  fmoles/cm<sup>2</sup>, and  $1.02 \pm 0.33$  fmoles/cm<sup>2</sup> for day 0, day 2, and day 4 respectively. This stability was contrasted by the variability of the 24 hour entrapment period which had surface concentrations of  $2.20 \pm 0.77$  fmoles/cm<sup>2</sup>,  $0.60 \pm 0.22$  fmoles/cm<sup>2</sup>,  $1.61 \pm 0.45$  fmoles/cm<sup>2</sup> for day 0, day 2, and day 4 respectively. An entrapment period of 48 hours showed a decreasing concentration of polyK from day 0 to day 6 with surface concentrations of  $1.60 \pm 0.37$  fmoles/cm<sup>2</sup>,  $1.09 \pm 0.26$  fmoles/cm<sup>2</sup>,  $0.35 \pm 0.10$  fmoles/cm<sup>2</sup>, and  $0.24 \pm 0.17$  fmoles/cm<sup>2</sup> respectively. Since stability was preferred over initial entrapment, all modified scaffolds were treated for 12 hours with the simple acetone and water solution containing polyK.

#### **1.4.4 Linking of fluorescent HE to films and fibers**

Fluorescently modified heparin was used to visually assess if the functionalized scaffold was further modified with GAG's, HE and HA, containing a carboxylic acid functional group. Modification was initially tested on PLA films and then PLA fibers. Control groups for the PLA films were plain PLA films with adsorbed heparin. PLA fibers were prepared using the previously stated procedures [57], then modified, and after modification the fibers mechanically separated to obtain interior fibers for fluorescent microscopy.



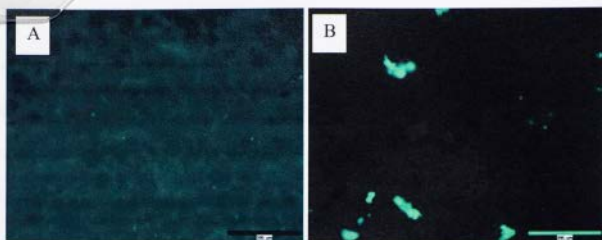



**Figure 7** Fluorescent micrographs, using an exposure time of 4000 ms, of the surface of PLA modified with the PA, polyK, linked to HE-FITC (left) and only incubated with HE-FITC showing HE physisorption (right). Both films were treated with heparin modified with EDC and NHS. The scale bar is 395  $\mu\text{m}$ .

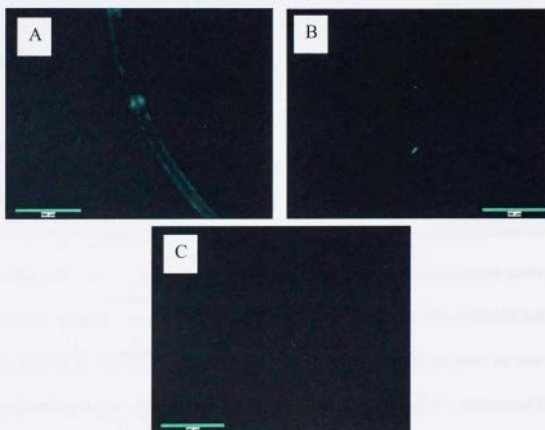


**Figure 8** PLA fiber scaffolds were modified with the PA, polyK, and linked to HE-FITC (A), only modified with the PA polyK (B), and only incubated with HE-FITC showing HE physisorption (C). The scale bar is 395  $\mu\text{m}$ .



The two control groups used were PLA fibers with only entrapped polyK and with only adsorbed HE. For both PLA films and fibers, higher fluorescence indicates biologically modified surfaces. Figure 7 shows the results for PLA films. A higher and uniform modification is seen in figure 7a while adsorbed heparin aggregates are shown on figure 7b.

Figure 8 shows the results for the PLA fibers. The fully modified fiber in figure 8a shows a higher fluorescence than figure 8b and figure 8c. It is important to note the lack of aggregates in figure 8b, and the lack of fluorescence of polyK in figure 8c. Additionally the fiber shown is intact, showing no damage from the acetone/water wash. This shows the higher fluorescence shown is from the covalently linked HE-FITC.

#### **1.4.5 Scaffold Cellularity**

Cellular response to both the physical entrapment and the biological modification was investigated. First, cells were statically seeded on scaffolds with HE or HA covalently linked to a PA, polyK, entrapped in the surface. Control groups of plain PLA or PLA with polyK entrapped. A phallotoxin was used to stain F-actin filaments and visualize the cells. These results are shown in figure 9. These results show stretched cells along the fiber surface as well as between fibers for fully modified scaffolds with HE in figure 9c. Scaffolds modified with HA showed a more round appearance as seen in figure 9d. Both control groups, plain PLA and PLA with entrapped polyK, contained few cells and rounded appearance.

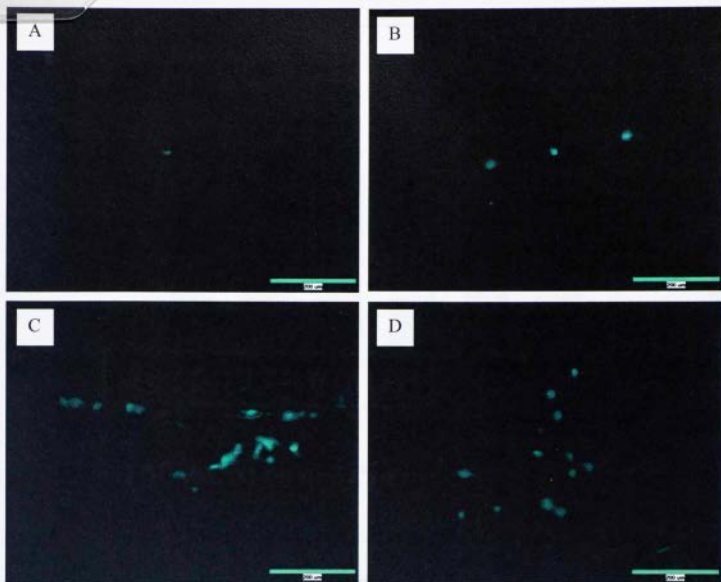



**Figure 9** Fluorescent micrographs, using an exposure time of 4000 ms, of statically seeded rMSCs showing the cellular shape taken on the surface of PLA modified with (A) nothing (B) polyK (C) HE (D) HA. Cellular F-actin filaments were stained using phalloidin. Scaffolds modified with HE or HA show cell stretching, while scaffolds with no modifications, or only polyK show limited stretching on the fiber surface. HE modified scaffolds show stretched cells along PLA fibers and across fibers. HA modified scaffolds show less stretched cells than heparin modified scaffolds, but more stretching than polyK modified scaffolds.

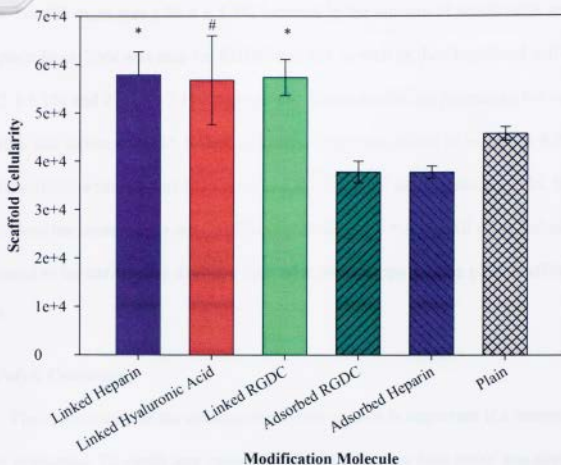


**Figure 10** Picogreen DNA assay results showing the scaffold cellularity with covalently linked to biological molecules, plain bars, versus scaffolds with adsorbed molecules and plain scaffolds, bars crosshatched. HE and HA were linked to the scaffold using a zero length carbodiimide linker and RGDC was linked using 6.8 Å spacer arm linker. Cell number was found from a picogreen DNA assay using the assumption of 7 pg/cell. (n =4, \* p<0.05 compared to control, # p>0.05 compared to the plain scaffold)

In order to quantify the effect of HE and HA modification, the scaffold cellularity, cells per scaffold, was found. This was done using picogreen DNA assay and a standard DNA content per cell of 7 pg/cell. The results are shown in figure 10. These results show an increase when biological molecules such as HE, HA, and RGDC are covalently linked to the surface of the polymer fibers and no increase when molecules are adsorbed to the



surface. For HE there was a  $26.4 \pm 7.5\%$  increase in the amount of attach cells compared to the plain fiber. This was true for RGDC and HA as well as they improved cell seeding by  $26.2 \pm 5.1\%$  and  $23.9 \pm 17.1\%$  respectively. These results are promising but some variability still exists with HA linked scaffolds. There was found to be  $56.7 \pm 9.2 \times 10^3$  cells/scaffold with HA linked to it and  $45.8 \pm 1.4 \times 10^3$  cells/ plain scaffold. Statistical tests showed the means were not significantly different,  $p = 0.09$ . All other linked groups were found to be statistically different than adsorbed groups and the plain scaffold,  $p < 0.05$ .

#### **1.4.6 PolyK Cytotoxicity**

The cytotoxicity of the entrapped polymer anchor is important if a material is to be later implanted. To verify any cytotoxic effects, an alamar blue assay was performed. Alamar blue assays are widely used in order to show the metabolic processes of cells are active and specifically the ability for cells to reduce resazurin. This nontoxic and cell permeable molecule is reduced to a fluorescent product, resorufin. This product can be measured and compared to a control cell group to deduce the viability of cells exposed to the polymer anchor. The assay performed here shows no difference statistically between the control and the modified group. The results are shown in figure 11. The control group had a value of  $1.3 \pm 0.033 \times 10^3$ , while the modified group had a value  $1.2 \pm 0.071 \times 10^3$  for the amount of resazurin reduced per cell. The viability of the modified cells was found to  $92.8 \pm 6.0\%$ . This result showed limited cytotoxicity of the polyK polymer to the cells over a short time period.

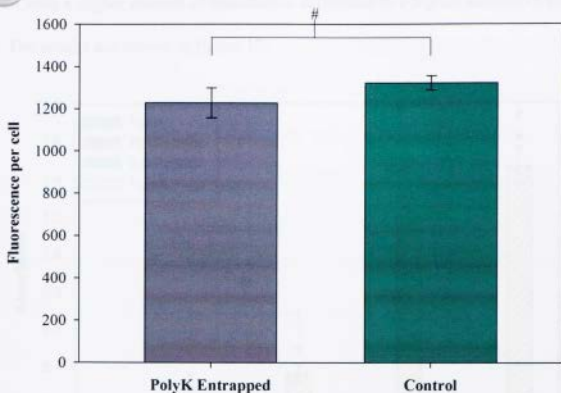


**Figure 11** The results are shown for the alamar blue assay for modified group, fiber scaffolds with polyK entrapped, and the control, no polyK entrapped. The results show negligible difference between the modified group and the control. Fluorescence was measured using an opaque white 96 – well plate and 300  $\mu$ L of each sample. The samples were measured at 530 nm excitation and 590 nm emission. (n = 3, p>0.05)

#### 1.4.7 PolyK Entrapment in Polymer Films

The polymer networks effect on the ability to entrap three different polymer anchors was tested. The polymer networks used were PCL, PLA, PLGA85, and PLGA50. The PAs were polyK, RL – peptide, PEG-amine. Each PA was tested separately at the same concentration. To measure the amount of entrapped polymer anchor, HRP and ABTS were used. This provided a qualitative estimate of the amount of polymer anchor

entrapped with a higher amount of absorbance correlated to a higher amount of polymer anchor. The results are shown in figure 12.

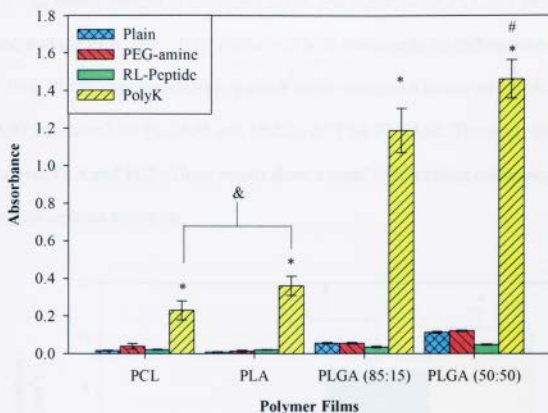


**Figure 12** The qualitative amount of different polymer anchors entrapped in PCL, PLA, PLGA (85:15), and PLGA (50:50). The amount of both entrapped polyK and percent amorphous increase from left to right. For each polymer, the amount of HRP covalently linked to a polyK was statistically higher than PEG-amine or RL-peptide. The amount of polyK also entrapped in PLGA85 and PLGA50 was statistically higher than PCL and PLA. (n=4, \* p<0.05, # highest absorbance, & p>0.05)

These results show a large increase between the highly crystalline PLA and the amorphous PLGA85. While polyK showed high entrapment amounts, the remaining hydrophilic polymer anchors did not. For each polymer film the amount of RL-peptide entrapped and PEG-amine entrapped was statistically lower than the amount of polyK,



and did not show higher amounts of HRP than the plain scaffolds. The quantified surface concentration in each of the four polymer networks using polyK as the PA is shown in figure 13. The lowest amount of entrapped polyK was found in the PCL at  $1.64 \pm 0.39$  fmole/cm<sup>2</sup> and the PLA  $2.67 \pm 0.39$  fmole/cm<sup>2</sup> with statistically no difference between the two. Both PLGA copolymers have a much larger amount of entrapped polyK, with  $8.60 \pm 0.90$  fmole/cm<sup>2</sup> for PLGA85 and  $10.22 \pm 0.77$  for PLGA50. These are 400% increases over PLA and PCL. These results show a trend of increasing entrapment with increasing amorphous structure.

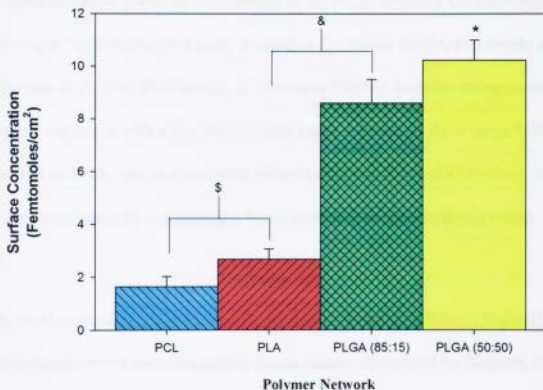


**Figure 13** The quantitative measurement of the amount of polyK entrapped into different poly ( $\alpha$ -hydroxy esters). There is an increase in the amount of the polyK entrapped in the highly amorphous structure of PLGA50 and PLGA85 (indicated by &), while the more crystalline structure of PLA and PCL showed lower entrapped polyK per cm<sup>2</sup>. The highest amount of entrapped polyK is shown by \*. (n = 4, \$ p > 0.05)





## 1.5 Discussion

This study presented a simple surface modification technique in order to introduce functional groups to the surface of commonly used biomaterials in tissue engineering applications. Surface modification can provide a functional surface that can then be linked to a variety of biological molecules. A surface modification technique for poly (L-lactic acid) scaffolds has been reported that utilizes an acetone/water solution and then DMSO to allow for the incorporation of polyK on the polymer surface. This study aimed at overcoming some negative effects that may be caused by the use of DMSO and the potential replacement of polyK to PEG-amine as the PA to improve the biocompatibility of this technique. Specifically this study wanted to 1) replace the PA previously used by Alvarez-Barreto et al. with PEG-amine, 2) eliminate DMSO from the entrapment procedure and replace it with a less biologically harsh solvent, 3) show large MW molecules, HE and HA, can be covalently linked to the surface, and 4) to show the versatility of the process by entrapping a PA in several poly ( $\alpha$  - hydroxy ester) polymers.

Physical entrapment is attractive for its low cost and simplicity. Originally, presented by Ruckenstein and Chung[58], it was further developed by Hubbell et al.[35]. That work presented the technique of creating a surface physical interpenetrating network (SPIN) through the use solvent trifluoroacetic acid. This allowed the surface of the polymer to swell and PEG to diffuse in. Then water was used to collapse the swollen network and entrap PEG. Specifically shown in this study was the effect the MW of the PA had on entrapment. The optimal PA was found to be 18.5 kDa with lower molecular weights not being exposed at the surface and higher molecular weights not sufficiently


entangled for diffusion out to be limited. Additionally the solvent and polymer used should optimally have a solubility factor with a difference squared no greater than 4, equation 1, for sufficient swelling to occur [36].

**Equation 1** 
$$(\delta_p - \delta_s)^2 < 4$$

In this equation,  $\delta_p$  is the solubility parameter in  $\text{cal}/\text{cm}^3$  of the polymer and  $\delta_s$  is the solubility parameter in  $\text{cal}/\text{cm}^3$  of the solvent. A variant of this method uses TFE and has the limitation using a strong solvent with a dermal  $\text{LD}_{50}$  of 1680 mg/kg in rats [59]. The  $\text{LD}_{50}$  is the median lethal dose needed to kill half a population sample after a certain period of time.


A less harsh method was created previously by Alvarez-Barreto et al. that used two steps to entrap a polymer anchor[41]. This method used acetone to swell the polymer surface, then DMSO to allow the polymer anchor to diffuse into the polymer network, and finally water to collapse the network. Alvarez-Barreto et al. were able to show uniform entrapment, covalent linking of the RGD tripeptide, and enhanced cellular attachment with osteoblastic induction using this method. While successful, this method still relies on a harsh solvent with DMSO, dermal  $\text{LD}_{50}$  of >5000 mg/kg in rabbits, and uses more steps than previous methods [60]. In order to improve this process, a simpler one step method, and a less harsh solvent (acetone), dermal  $\text{LD}_{50}$  of 7426 mg/kg in guinea pigs, was used [61].

Acetone is a cheap, versatile solvent with a compatible solubility factor, 19.93  $\text{MPa}^{1/2}$ , for use with PLA, 21.01  $\text{MPa}^{1/2}$  [62]. Because of the aforementioned features of acetone, it was chosen as an investigatory solvent to replace DMSO as the solvent beyond its already established use as a swelling agent. To test the acetone/water solution,



two methods were used. Method (1) acted as a control, (by using the same procedure as Alvarez-Barreto et al.) using acetone/water to swell the polymer and DMSO with the PA for entrapment, and method (2) used the simpler acetone/water solution with the PA for entrapment. Additionally, a 20kDa PEG-amine was chosen to satisfy the results shown by Hubbel et al. The results of using the method (1) and method (2) are shown in figure 3. The simple one step procedure is shown to produce a modified surface with over 5 times the surface concentration of polyK entrapped. This result was unexpected as it was not in agreement with results reported by Alvarez-Barreto et al. with a PLLA polymer network.


DMSO was initially used for its excellent solvent capability when dissolving the polyK used in this experiment, and its hypothesized slowing of the collapse of the polymer network[40]. This simultaneous interaction with the polymer network and the PA allowed for an increased amount of entrapment over method (2) in the previous study. This was not the case in this investigation where instead of pure PLLA, the poly (lactic acid) contained 1.49% of the D enantiomer decreasing the polymer's crystallinity. The difference in polymer networks was substantial. It is thought the swelling of the polymer is much slower using PLA with slight D impurities. Figure 6 shows that increased entrapment time can increase the amount of PA entrapped. This proves that time does have an effect on the entrapment. While the swelling time is adequate for method (2), 12 hours, it is inadequate for method (1), 1 hour. This lack of swelling caused the PA to not adequately diffuse into the polymer network, and thus being not effectively entrapped. Because of this, the potential benefits of increased PA entrapment when using method (1) was negligible and method (2) was used throughout the rest of the experiment.



Another key feature of figure 3 is the lack of entrapment when PEG-amine as PA. Past investigations involving the entrapment of hydrophilic PA into hydrophobic polymer networks have used the polar solvent, TFE [63]. Its polar nature is hypothesized to interact strongly with both the polymer anchor and the polymer network equally, while acetone preferentially interacts with the polymer network. This interaction leads the polymer anchor to interact highly with the water, and therefore to stay in the solution instead of diffusing into the polymer network.

The extent of this interaction was investigated in section 1.3.12 and can be seen in figure 12. While polyK was entrapped in increasing amounts in the PCL, PLA, PLGA85, and PLGA50, the PAs with hydrophilic characteristics, PEG-amine and RL-peptide, were not statistically different than control. For both of these PAs dissolution was complete in the acetone/water solution but entrapment was inadequate. Because dissolution is not a variable for PEG-amine and RL-peptide, the interaction between the solvent, polymer network, and the PA is effecting the entrapment. PolyK is a hydrophobic polymer and doesn't interact with the acetone/water solution highly, shown by the lack of complete dissolution, but it did entrap at a higher surface concentration than both PEG-amine and RL-peptide. These results, shown in figure 12, show a link between the hydrophobicity of the polymer and the amount of entrapped material.


The sustainability of the modification is important for long term effects. This was tested by measuring the amount of HRP that was covalently linked to polyK after a certain number of days. It was deemed to have no polyK left entrapped after the absorbance was the same as the control group. Figure 6 shows these results for time periods of entrapment of 12, 24, and 48 hours. While 24 hours has the largest initial



entrapment, the polyK quickly diffuses out over a six day time period. The 48 hour time period showed a slightly higher amount than the 12 hour time period and less than the 24 hour time period. While none of the time periods show long term stability, the initial stability shown by the entrapment time period of 12 hours over the six day time period makes this most suitable for longer term cultures where a stable biomimetic surface is needed to signal cells to deposit matrix. By the sixth day cells have begun ECM deposition and signaling nearby cells themselves not requiring the underlying biomimetic surface [64-68].

The instability of this entrapment method is unique, and provides that special precautions must be made. Previous studies have shown stable entrapment. Alvarez-Barreto et al. showed stability over ten days, while Quirk et al. and Hubbell et al. washed samples for extended periods, up to two weeks, to ensure leachables were negligible. Because of the instability, the turnaround time between the modification and the final application must be limited to four to six days. Leaching of remnants from the entrapment procedure is of high importance. Figure 11 shows the results of the cytotoxicity assay. The modified scaffold seeded statically showed a  $92.78 \pm 5.97\%$  viability compared to a plain scaffold after a two day culture. It was important that the scaffolds be modified and for the PA not to leach out into the solution for this experiment. This allows the cells to interact with the peptide on the surface as it would *in vivo*. Additionally, leaching of any solvents would also show by a decrease in viability of the cells. These results show that the effects of leachables as well as the modified polyK are shown to be negligible [69, 70].






Quirk et al. were the first to explore PLA as a polymer network for physical entrapment, and were able to successfully entrap poly (L-lysine) and PEG. Using a method with 10% TFE, they were able to successfully entrap PEG and poly (L-lysine) simultaneously, proving the method is able to entrap different polymers and with different functional groups simultaneously. While successfully modifying the surface, the method did produce non-uniformity on the surface in certain conditions[38].

A uniform surface is important for a biological signal to be evenly distributed over the surface of the material. Figure 2 shows the results testing the uniformity of the entrapment of polyK. The darker areas observable on the PLA films shown in figure 4a are shown to be abnormalities of the polymer network, instead of areas of low entrapment, by figure 7a. These results show that a uniform signal will be given to the cells, no matter the position of attachment, providing an excellent background for enhancing cellular attachment, proliferation, and differentiation through the attachment of growth factors and ECM peptides. This allows for control over initial cell packing, growth rate, and the final tissue product, three important factors for tissue engineering.


Covalent attachment is a versatile way for biological molecules to be attached to a functionalized surface. This method is robust enough that for any functional group the appropriate linker is available [71-75]. For covalent attachment of GAG's an appropriate linker is the carbodiimide, EDC, stabilized with NHS. This molecule reacts efficiently with the carboxylic acid available on all abundant GAG's and can be readily reacted with a free amine on another molecule[76-80]. This functionalization does hydrolyze and return to a carboxylic acid if not reacted quickly. The NHS stabilizes the functionality for longer storage[81]. Both HE and HA were functionalized and covalently attached to the



surface of both polymer films. The results of attaching a fluorescent HE are shown in figure 7 and 8. It is assumed that HA, with its similar structure, attaches similarly. In figure 7a it can be seen that HE attaches uniformly across the surface. Aggregates of HE can be seen in figure 7b. This phenomenon is hypothesized to be a function of small holes etched by the extended use of the acetone/water solution of method (2) in the PLA films. Aggregates of HE are formed and stabilized in the holes, not being washed out during the standard rinsing. It is seen when given adequate functionalities to react on the surface, aggregation is stopped and the surface does not have clumps of HE.


Three dimensional scaffolds and specifically fiber scaffolds have beneficial characteristics for tissue engineering, such as increased cell attachment, matrix deposition, and tissue organization [82-84]. An important characteristic of a well modified scaffold is uniform entrapment throughout the scaffold and an intact porous network. The porous network allows for adequate nutrient distribution within the scaffold which facilitates cell proliferation, uniform differentiation, and leads to a healthier engineered tissue. Fiber scaffolds were created via melt blowing, with fiber diameters of 35  $\mu\text{m}$ , and arranged in a non-woven pattern. These fibers were then modified for the specified amount of time and then imaged for any damage to fibers. The fibers are shown in figure 8, with fluorescently modified HE attached to the surface. It can be seen that no deformation is shown in the fibers (figure 8a), polyK does not fluoresce (figure 8b), and that HE is attached uniformly along a fibers length (figure 8a). This shows uniform entrapment and uniform modification along the fiber, without destruction of the fibers and therefore the porous network.





RGD is one of a family of peptides that are derived from proteins found in the ECM. These include the YIGSR and REDV peptides from laminin and fibronectin respectively that have been shown to increase cell adhesion [85, 86]. This tripeptide has been shown to increase the attachment of multiple cell types, and to also affect stem cell differentiation. Several different possible routes for the attachment of the tripeptide have been shown. An important aspect of this is that the peptide should have an appropriate distance from the surface for optimal attachment. To impart this space a dual functionalized linker was used to react to the free surface amine and the thiol group of the carboxyl end cysteine of RGDC. This method was shown and described previously by Alvarez-Barreto et al. Quantitative measurements are possible when using SPDP because of the release of the pyridine - 2 - thione group when SPDP is reacted with a molecule containing a thiol functional group. The amount of polyK and therefore SPDP linked to the surface during this experiment falls below the detection limit as found by Alvarez-Barreto et al. The previous study found a limit at  $18 \pm 6$  nmoles of SPDP or less than 60 pg of polyK. The amount of entrapped polyK in the current study was found to be  $34.32 \pm 4.06$  pg, which is lower than the detectable limit. Because of this, the effect on cell attachment was chosen to corroborate the linking of RGDC.

Cell attachment is very important to tissue engineering in order to decrease the amount of time for a mature tissue to be created. To this end, the fiber scaffolds were modified and statically cultured in order to investigate increased attachment. First cell shape was investigated using fluorescent microscopy. The shape the cell takes when attaching to a material indicates the level of efficient surface modification, and therefore can be used to show the strength of attachment. Figure 9 shows the fluorescently stained



cells attaching to fibers. Figure 9c and figure 9d show larger cell shapes indicating more of the cell is in contact with the fiber. In contrast, figure 9a and 9b show the cell shapes taken on plain fibers or fibers with only polyK respectively.

All of the fully modified scaffolds showed an increase in level of cell attachment, approximately 25% increase for each, as shown in figure 10. These results concur with recent results. RGD was adsorbed to a chitosan/hydroxyapatite scaffold at two different concentrations and showed an increase in cellular adhesion of 30.9% and 47.5% respectively [87]. Previous results from Alvarez-Barreto concur with the results shown in figure 10 for RGD by showing an increase in attachment when using RGD [42]. The increase cellularity for that study is found to be much larger than shown here. A rule of thumb was found by Massia and Hubbell, that the minimum amount of RGD peptide sufficient for cell spreading was  $1 \text{ fmol/cm}^2$  and as low as  $10 \text{ fmol/cm}^2$  to begin the formation of focal contacts and stress fibers [88]. This has been shown to vary for different surfaces but generally has been shown to have increased values [89-92]. Entrapment of polyK in PLA showed a surface concentration of  $1 \pm 0.15 \text{ fmoles/cm}^2$ , seen in figure 3. This by itself falls below the rule established by Massia and Hubbell with the assumption of 100% reaction yield of SPDP with polyK and 100% reaction yield of RGDC with SPDP. Because yields of that magnitude may not occur, the results of only a marginal increase are explained.

Poly ( $\alpha$ -hydroxy esters) are versatile polymers used to create scaffolds for several different tissue types. Because of their importance, the physical entrapment of a PA into several different polymers of that family was investigated. These included PCL and PLGA. Copolymers of PLA and PGA have been useful because different ratios of


polymers have shown to have wide range of mechanical and degradation properties.

Figure 12 shows the results of physical entrapment with several different polymers.

Important characteristics shown in the figure are the steep increase when the polymers become highly amorphous from PLA to PLGA85. PCL has been shown to have a crystallinity of approximately 50% [93], while PLA is semi-crystalline with the addition of the D isomer. This is increased in PLGA85 and PLGA50 with the addition of glycolic acid and the 50:50 ratio of D to L lactic acid isomers. These results show for the first time that the increase in amorphous structure improves the ability for polyK to be entrapped. The solubility parameters also show an increase as PLA is blended into PGA [94]. This allows for the entrapment of polyK to be controlled by the polymer network chosen. With PLGA85 and PLGA50 the amount of polyK entrapped was approximately 400% times higher than PLA or PCL. This entrapment is also higher than those shown by Alvarez – Barreto et al. in the previous study, with  $275.91 \pm 19.23$  pg and  $58.5 \pm 0.5$  pg respectively.

**Table 1** Representative crystallinity values for poly ( $\alpha$  – hydroxy ester) polymers used in this study.


Polymer	Crystallinity	Notes	Reference
Poly(L-lactic acid)	$57 \pm 5$ %	100% L enantiomer	[95]
Poly(D,L Lactic acid)	44 %	94% L and 6% d enantiomer	[95]
Poly ( $\epsilon$ -caprolactone)	$50 \pm 1$ %	-	[96]
poly (D,L – lactide – co – glycolide) [85:15]	amorphous	-	[97]
poly (D,L – lactide – co – glycolide) [50:50]	amorphous	-	[97]




Included in section 1.4.7 is figure 11, which shows the use of a three peptides with a range of hydrophobic or hydrophilic properties. The most hydrophilic polymer anchor is PEG-amine, while the custom peptide, RL-peptide, is a di-block polymer with half hydrophobic amino acids, leucine, and half hydrophilic amino acids, arginine, and polyK was used for the fully hydrophobic peptide. This graph shows that the only polymer anchor to substantially entrap is the polyK. As described previously, this is hypothesized to be because of the solvent – polymer anchor and water-polymer anchor interactions. These results further explore this by showing that increased hydrophobicity is needed to enable entrapment. Because this process increases the polymer anchor and the polymer network interactions so much, these direct interactions should be investigated to completely understand this behavior. The hydrophobic nature of the polymer anchor and the side chain of the amino acid, specifically the benzene ring, should be investigated to better understand the method of entrapping the polyK.

## 1.6 Conclusion

This investigation presents a simple, versatile method for the introduction of functional groups to the surface of polymers networks. The networks can include both 2-D structures, such as films, and 3-D structures, such as fibers. Initial attempts to replace polyK with a more widely used polymer, PEG-amine, was unsuccessful. This is thought to be because of interactions between the solvent solution and the PA during entrapment. Previously used solvents were replaced with an acetone/water solution and a simple one step method was performed. This modification was shown to be uniform over the surface, but unstable over time. Modification to fibers was shown at biologically relevant concentrations to increase in cell attachment to all fully modified scaffolds by as much as





25% when using HE, HA, and RGD. This process can easily be extended to other biological molecules for tissue engineering or other material based scenarios by simply applying the correct linking mechanism to the appropriate functional groups.


The extension of this process to other poly ( $\alpha$ -hydroxy ester) polymer networks further shows its versatility and expands its use to several different biomaterials and tissue engineering applications. Two generalizations have also been shown by this investigation. The interactions between the solvent solution, the polymer network, and the polymer anchor are important to the entrapment process. We have shown that more than 50% of the polymer must be hydrophilic and possible as much as 100%. This should be investigated further in order to understand this in greater detail. Second, the process can be controlled to a degree by the amount of time the PA is entrapped and by using a more amorphous structure. The latter showing more defining and controllable characteristics.



## 1.7 References


1. Langer, R. and J.P. Vacanti, *TISSUE ENGINEERING*. Science, 1993. **260**(5110): p. 920-926.
2. Chamberlain, G., et al., *Concise review: Mesenchymal stem cells: Their phenotype, differentiation capacity, immunological features, and potential for homing*. Stem Cells, 2007. **25**(11): p. 2739-2749.
3. Tuan, R.S., G. Boland, and R. Tuli, *Adult mesenchymal stem cells and cell-based tissue engineering*. Arthritis Research & Therapy, 2003. **5**(1): p. 32-45.
4. Wang, H.S., et al., *Mesenchymal stem cells in the Wharton's jelly of the human umbilical cord*. Stem Cells, 2004. **22**(7): p. 1330-1337.
5. Ringe, J., et al., *Stem cells for regenerative medicine: advances in the engineering of tissues and organs*. Naturwissenschaften, 2002. **89**(8): p. 338-351.
6. He, L.J., et al., *Full-thickness tissue engineered skin constructed with autogenic bone marrow mesenchymal stem cells*. Science in China Series C-Life Sciences, 2007. **50**(4): p. 429-437.
7. Liu, P., et al., *Tissue-Engineered Skin Containing Mesenchymal Stem Cells Improves Burn Wounds*. Artificial Organs, 2008. **32**(12): p. 925-931.
8. Arinze, T.L., et al., *Allogeneic mesenchymal stem cells regenerate bone in a critical-sized canine segmental defect*. Journal of Bone and Joint Surgery-American Volume, 2003. **85A**(10): p. 1927-1935.
9. Zhou, J., et al., *The repair of large segmental bone defects in the rabbit with vascularized tissue engineered bone*. Biomaterials, 2010. **31**(6): p. 1171-1179.
10. Hillel, A.T., et al., *Characterization of Human Mesenchymal Stem Cell-Engineered Cartilage: Analysis of Its Ultrastructure, Cell Density and Chondrocyte Phenotype Compared to Native Adult and Fetal Cartilage*. Cells Tissues Organs, 2010. **191**(1): p. 12-20.
11. Li, W.J., et al., *A three-dimensional nanofibrous scaffold for cartilage tissue engineering using human mesenchymal stem cells*. Biomaterials, 2005. **26**(6): p. 599-609.




- 
12. Wang, L., et al., *Differentiation of human bone marrow mesenchymal stem cells grown in terpolyesters of 3-hydroxyalkanoates scaffolds into nerve cells*. *Biomaterials*, 2010. **31**(7): p. 1691-1698.
  13. Prabhakaran, M.P., J.R. Venugopal, and S. Ramakrishna, *Mesenchymal stem cell differentiation to neuronal cells on electrospun nanofibrous substrates for nerve tissue engineering*. *Biomaterials*, 2009. **30**(28): p. 4996-5003.
  14. Ramaswamy, S., et al., *The role of organ level conditioning on the promotion of engineered heart valve tissue development in-vitro using mesenchymal stem cells*. *Biomaterials*, 2010. **31**(6): p. 1114-1125.
  15. Engelmayr, G.C., et al., *Cyclic flexure and laminar flow synergistically accelerate mesenchymal stem cell-mediated engineered tissue formation: Implications for engineered heart valve tissues*. *Biomaterials*, 2006. **27**(36): p. 6083-6095.
  16. Lutolf, M.P. and J.A. Hubbell, *Synthetic biomaterials as instructive extracellular microenvironments for morphogenesis in tissue engineering*. *Nature Biotechnology*, 2005. **23**(1): p. 47-55.
  17. Burdick, J.A. and G. Vunjak-Novakovic, *Engineered Microenvironments for Controlled Stem Cell Differentiation*. *Tissue Engineering Part A*, 2009. **15**(2): p. 205-219.
  18. Stevens, M.M. and J.H. George, *Exploring and engineering the cell surface interface*. *Science*, 2005. **310**(5751): p. 1135-1138.
  19. Place, E.S., N.D. Evans, and M.M. Stevens, *Complexity in biomaterials for tissue engineering*. *Nature Materials*, 2009. **8**(6): p. 457-470.
  20. Hench, L.L. and J.M. Polak, *Third-generation biomedical materials*. *Science*, 2002. **295**(5557): p. 1014-+.
  21. Ulerý, B.D., L.S. Nair, and C.T. Laurencin, *Biomedical Applications of Biodegradable Polymers*. *Journal of Polymer Science Part B-Polymer Physics*, 2011. **49**(12): p. 832-864.
  22. Yang, S.F., et al., *The design of scaffolds for use in tissue engineering. Part I. Traditional factors*. *Tissue Engineering*, 2001. **7**(6): p. 679-689.




23. Ishaug, S.L., et al., *Bone formation by three-dimensional stromal osteoblast culture in biodegradable polymer scaffolds*. Journal of Biomedical Materials Research, 1997. **36**(1): p. 17-28.
24. Shin, H., S. Jo, and A.G. Mikos, *Biomimetic materials for tissue engineering*. Biomaterials, 2003. **24**(24): p. 4353-4364.
25. Ma, P.X., *Biomimetic materials for tissue engineering*. Advanced Drug Delivery Reviews, 2008. **60**(2): p. 184-198.
26. Cai, Q., et al., *Biomimetic mineralization of electrospun poly(L-lactic acid)/gelatin composite fibrous scaffold by using a supersaturated simulated body fluid with continuous CO<sub>2</sub> bubbling*. Applied Surface Science, 2011. **257**(23): p. 10109-10118.
27. Zhang, D.M., J. Chang, and Y. Zeng, *Fabrication of fibrous poly(butylene succinate)/wollastonite/apatite composite scaffolds by electrospinning and biomimetic process*. Journal of Materials Science-Materials in Medicine, 2008. **19**(1): p. 443-449.
28. Tran, N.Q., et al., *RGD-conjugated In Situ forming hydrogels as cell-adhesive injectable scaffolds*. Macromolecular Research, 2011. **19**(3): p. 300-306.
29. Mi, F.L., et al., *Fabrication of chondroitin sulfate-chitosan composite artificial extracellular matrix for stabilization of fibroblast growth factor*. Journal of Biomedical Materials Research Part A, 2006. **76A**(1): p. 1-15.
30. Ding, Z., et al., *Immobilization of chitosan onto poly-L-lactic acid film surface by plasma graft polymerization to control the morphology of fibroblast and liver cells*. Biomaterials, 2004. **25**(6): p. 1059-1067.
31. Zhu, A.P., et al., *Adhesion contact dynamics of 3T3 fibroblasts on poly (lactide-co-glycolide acid) surface modified by photochemical immobilization of biomacromolecules*. Biomaterials, 2006. **27**(12): p. 2566-2576.
32. Liston, E.M., L. Martinu, and M.R. Wertheimer, *PLASMA SURFACE MODIFICATION OF POLYMERS FOR IMPROVED ADHESION - A CRITICAL-REVIEW*. Journal of Adhesion Science and Technology, 1993. **7**(10): p. 1091-1127.
33. Yang, X.B., et al., *Human osteoprogenitor growth and differentiation on synthetic biodegradable structures after surface modification*. Bone, 2001. **29**(6): p. 523-531.


- 
34. Zhu, Y.B., et al., *Surface modification of polycaprolactone membrane via aminolysis and biomacromolecule immobilization for promoting cytocompatibility of human endothelial cells*. *Biomacromolecules*, 2002. **3**(6): p. 1312-1319.
35. Desai, N.P. and J.A. Hubbell, *SOLUTION TECHNIQUE TO INCORPORATE POLYETHYLENE OXIDE AND OTHER WATER-SOLUBLE POLYMERS INTO SURFACES OF POLYMERIC BIOMATERIALS*. *Biomaterials*, 1991. **12**(2): p. 144-153.
36. Desai, N.P. and J.A. Hubbell, *SURFACE PHYSICAL INTERPENETRATING NETWORKS OF POLY(ETHYLENE-TEREPHTHALATE) AND POLY(ETHYLENE OXIDE) WITH BIOMEDICAL APPLICATIONS*. *Macromolecules*, 1992. **25**(1): p. 226-232.
37. Quirk, R.A., et al., *Surface engineering of poly(lactic acid) by entrapment of modifying species*. *Macromolecules*, 2000. **33**(2): p. 258-260.
38. Quirk, R.A., et al., *Characterization of the spatial distributions of entrapped polymers following the surface engineering of poly(lactic acid)*. *Surface and Interface Analysis*, 2001. **31**(1): p. 46+.
39. Hou, Q.P., et al., *Novel surface entrapment process for the incorporation of bioactive molecules within preformed alginate fibers*. *Biomacromolecules*, 2005. **6**(2): p. 734-740.
40. Alvarez-Barreto, J.F., et al., *Preparation of a functionally flexible, three-dimensional, biomimetic poly(L-lactic acid) scaffold with improved cell adhesion*. *Tissue Engineering*, 2007. **13**(6): p. 1205-1217.
41. Alvarez-Barreto, J.F., et al., *Enhanced osteoblastic differentiation of mesenchymal stem cells seeded in RGD-functionalized PLLA scaffolds and cultured in a flow perfusion bioreactor*. *Journal of Tissue Engineering and Regenerative Medicine*, 2011. **5**(6): p. 464-475.
42. Alvarez-Barreto, J.F. and V.I. Sikavitsas, *Improved mesenchymal stem cell seeding on RGD-modified poly(L-lactic acid) scaffolds using flow perfusion*. *Macromolecular Bioscience*, 2007. **7**(5): p. 579-588.
43. Chen, W.Y.J. and G. Abatangelo, *Functions of hyaluronan in wound repair*. *Wound Repair and Regeneration*, 1999. **7**(2): p. 79-89.

44. Toole, B.P., *Hyaluronan: From extracellular glue to pericellular cue*. Nature Reviews Cancer, 2004. **4**(7): p. 528-539.
45. Culty, M., et al., *THE HYALURONATE RECEPTOR IS A MEMBER OF THE CD44 (H-CAM) FAMILY OF CELL-SURFACE GLYCOPROTEINS*. Journal of Cell Biology, 1990. **111**(6): p. 2765-2774.
46. Hall, C.L., et al., *HYALURONAN AND THE HYALURONAN RECEPTOR RHAMM PROMOTE FOCAL ADHESION TURNOVER AND TRANSIENT TYROSINE KINASE-ACTIVITY*. Journal of Cell Biology, 1994. **126**(2): p. 575-588.
47. Gao, F., et al., *Hyaluronan oligosaccharides promote excisional wound healing through enhanced angiogenesis*. Matrix Biology, 2010. **29**(2): p. 107-116.
48. Matou-Nasri, S., et al., *Oligosaccharides of hyaluronan induce angiogenesis through distinct CD44 and RHAMM-mediated signalling pathways involving Cdc2 and gamma-adducin*. International Journal of Oncology, 2009. **35**(4): p. 761-773.
49. Pilarski, L.M., et al., *Potential role for hyaluronan and the hyaluronan receptor RHAMM in mobilization and trafficking of hematopoietic progenitor cells*. Blood, 1999. **93**(9): p. 2918-2927.
50. Baldwin, A.D. and K.L. Kiick, *Polysaccharide-Modified Synthetic Polymeric Biomaterials*. Biopolymers, 2010. **94**(1): p. 128-140.
51. Singh, S., B.M. Wu, and J.C.Y. Dunn, *The enhancement of VEGF-mediated angiogenesis by polycaprolactone scaffolds with surface cross-linked heparin*. Biomaterials, 2011. **32**(8): p. 2059-2069.
52. Sakiyama-Elbert, S.E. and J.A. Hubbell, *Controlled release of nerve growth factor from a heparin-containing fibrin-based cell ingrowth matrix*. Journal of Controlled Release, 2000. **69**(1): p. 149-158.
53. Jeon, O., et al., *Affinity-based growth factor delivery using biodegradable, photocrosslinked heparin-alginate hydrogels*. Journal of Controlled Release, 2011. **154**(3): p. 258-266.
54. Capila, I. and R.J. Linhardt, *Heparin - Protein interactions*. Angewandte Chemie-International Edition, 2002. **41**(3): p. 391-412.

- 
55. Noël, S., et al., *Quantification of Primary Amine Groups Available for Subsequent Biofunctionalization of Polymer Surfaces*. *Bioconjugate Chemistry*, 2011. **22**(8): p. 1690-1699.
56. Issa, R.I., et al., *The Effect of Cell Seeding Density on the Cellular and Mechanical Properties of a Mechanostimulated Tissue-Engineered Tendon*. *Tissue Engineering Part A*, 2011. **17**(11-12): p. 1479-1487.
57. VanGordon, S.B., et al., *Effects of Scaffold Architecture on Preosteoblastic Cultures under Continuous Fluid Shear*. *Industrial & Engineering Chemistry Research*, 2011. **50**(2): p. 620-629.
58. Ruckenstein, E. and D.B. Chung, *SURFACE MODIFICATION BY A 2-LIQUID PROCESS DEPOSITION OF A-B-BLOCK COPOLYMERS*. *Journal of Colloid and Interface Science*, 1988. **123**(1): p. 170-185.
59. *2,2,2 - Trifluoroethanol*. 2012, Sigma-Aldrich.
60. *Dimethyl Sulfoxide*. 2012, Sigma - Aldrich.
61. *Acetone*. 2012, Sigma-Aldrich.
62. Siemann, U., *THE SOLUBILITY PARAMETER OF POLY(DL-LACTIC ACID)*. *European Polymer Journal*, 1992. **28**(3): p. 293-297.
63. Meng, B., et al., *A new method of heparinizing PLLA film by surface entrapment*. *Journal of Bioactive and Compatible Polymers*, 2004. **19**(2): p. 131-143.
64. Mahmood, T.A., et al., *Tissue engineering of bovine articular cartilage within porous poly(ether ester) copolymer scaffolds with different structures*. *Tissue Engineering*, 2005. **11**(7-8): p. 1244-1253.
65. Mauck, R.L., et al., *Regulation of cartilaginous ECM gene transcription by chondrocytes and MSCs in 3D culture in response to dynamic loading*. *Biomechanics and Modeling in Mechanobiology*, 2007. **6**(1-2): p. 113-125.

- 
66. Nikolaev, N.I., et al., *A Validated Model of GAG Deposition, Cell Distribution, and Growth of Tissue Engineered Cartilage Cultured in a Rotating Bioreactor*. Biotechnology and Bioengineering, 2010. **105**(4): p. 842-853.
67. Bancroft, G.N., et al., *Fluid flow increases mineralized matrix deposition in 3D perfusion culture of marrow stromal osteoblasts in a dose-dependent manner*. Proceedings of the National Academy of Sciences of the United States of America, 2002. **99**(20): p. 12600-12605.
68. Farrell, E., et al., *A collagen-glycosaminoglycan scaffold supports adult rat mesenchymal stem cell differentiation along osteogenic and chondrogenic routes*. Tissue Engineering, 2006. **12**(3): p. 459-468.
69. Pinto, S., et al., *Poly(dimethyl siloxane) surface modification by low pressure plasma to improve its characteristics towards biomedical applications*. Colloids and Surfaces B-Biointerfaces, 2010. **81**(1): p. 20-26.
70. Liu, H.F., et al., *Modification of sericin-free silk fibers for ligament tissue engineering application*. Journal of Biomedical Materials Research Part B-Applied Biomaterials, 2007. **82B**(1): p. 129-138.
71. Jentoft, N. and D.G. Dearborn, *LABELING OF PROTEINS BY REDUCTIVE METHYLATION USING SODIUM CYANOBOROHYDRIDE*. Journal of Biological Chemistry, 1979. **254**(11): p. 4359-4365.
72. Levesque, S.G. and M.S. Shoichet, *Synthesis of enzyme-degradable, peptide-cross-linked dextran hydrogels*. Bioconjugate Chemistry, 2007. **18**(3): p. 874-885.
73. Lomant, A.J. and G. Fairbanks, *CHEMICAL PROBES OF EXTENDED BIOLOGICAL STRUCTURES - SYNTHESIS AND PROPERTIES OF CLEAVABLE PROTEIN CROSS-LINKING REAGENT DITHIOBIS(SUCCINIMIDYL-S-35 PROPIONATE)*. Journal of Molecular Biology, 1976. **104**(1): p. 243-261.
74. Kluger, R. and A. Alagic, *Chemical cross-linking and protein-protein interactions - a review with illustrative protocols*. Bioorganic Chemistry, 2004. **32**(6): p. 451-472.
75. Mullins, R.D., W.F. Stafford, and T.D. Pollard, *Structure, subunit topology, and actin-binding activity of the Arp2/3 complex from Acanthamoeba*. Journal of Cell Biology, 1997. **136**(2): p. 331-343.



- 
76. Pieper, J.S., et al., *Preparation and characterization of porous crosslinked collagenous matrices containing bioavailable chondroitin sulphate*. *Biomaterials*, 1999. **20**(9): p. 847-858.
77. Kim, J., et al., *Protein immobilization on plasma-polymerized ethylenediamine-coated glass slides*. *Analytical Biochemistry*, 2003. **313**(1): p. 41-45.
78. Rafat, M., et al., *PEG-stabilized carbodiimide crosslinked collagen-chitosan hydrogels for corneal tissue engineering*. *Biomaterials*, 2008. **29**(29): p. 3960-3972.
79. Bertrand, R., et al., *CROSS-LINKING OF THE SKELETAL MYOSIN SUBFRAGMENT-1 HEAVY-CHAIN TO THE N-TERMINAL ACTIN SEGMENT OF RESIDUES 40-113*. *Biochemistry*, 1988. **27**(15): p. 5728-5736.
80. Mercuri, J.J., et al., *Glycosaminoglycan-targeted fixation for improved bioprosthetic heart valve stabilization*. *Biomaterials*, 2007. **28**(3): p. 496-503.
81. Girardot, J.M.D. and M.N. Girardot, *Amide cross-linking: An alternative to glutaraldehyde fixation*. *Journal of Heart Valve Disease*, 1996. **5**(5): p. 518-525.
82. Barralet, J.E., et al., *Comparison of bone marrow cell growth on 2D and 3D alginate hydrogels*. *Journal of Materials Science-Materials in Medicine*, 2005. **16**(6): p. 515-519.
83. Dhiman, H.K., A.R. Ray, and A.K. Pan̄la, *Three-dimensional chitosan scaffold-based MCF-7 cell culture for the determination of the cytotoxicity of tamoxifen*. *Biomaterials*, 2005. **26**(9): p. 979-986.
84. Zare-Mehrjardi, N., et al., *Differentiation of embryonic stem cells into neural cells on 3D poly (D, L-lactic acid) scaffolds versus 2D cultures*. *International Journal of Artificial Organs*, 2011. **34**(10): p. 1012-1023.
85. Hubbell, J.A., et al., *ENDOTHELIAL CELL-SELECTIVE MATERIALS FOR TISSUE ENGINEERING IN THE VASCULAR GRAFT VIA A NEW RECEPTOR*. *Bio-Technology*, 1991. **9**(6): p. 568-572.
86. Ranieri, J.P., et al., *NEURONAL CELL ATTACHMENT TO FLUORINATED ETHYLENE-PROPYLENE FILMS WITH COVALENTLY IMMOBILIZED LAMININ*



OLIGOPEPTIDES YIGSR AND IKVAV.2. Journal of Biomedical Materials Research, 1995. **29**(6): p. 779-785.

87. Qu, Z.W., et al., *Improving bone marrow stromal cell attachment on chitosan/hydroxyapatite scaffolds by an immobilized RGD peptide*. Biomedical Materials, 2010. **5**(6).

88. Massia, S.P. and J.A. Hubbell, *AN RGD SPACING OF 440NM IS SUFFICIENT FOR INTEGRIN ALPHA-V-BETA-3-MEDIATED FIBROBLAST SPREADING AND 140NM FOR FOCAL CONTACT AND STRESS FIBER FORMATION*. Journal of Cell Biology, 1991. **114**(5): p. 1089-1100.

89. Elbert, D.L. and J.A. Hubbell, *Conjugate addition reactions combined with free-radical cross-linking for the design of materials for tissue engineering*. Biomacromolecules, 2001. **2**(2): p. 430-441.

90. Neff, J.A., P.A. Tresco, and K.D. Caldwell, *Surface modification for controlled studies of cell-ligand interactions*. Biomaterials, 1999. **20**(23-24): p. 2377-2393.

91. Drumheller, P.D., D.L. Elbert, and J.A. Hubbell, *MULTIFUNCTIONAL POLY(ETHYLENE GLYCOL) SEMIINTERPENETRATING POLYMER NETWORKS AS HIGHLY SELECTIVE ADHESIVE SUBSTRATES FOR BIOADHESIVE PEPTIDE GRAFTING*. Biotechnology and Bioengineering, 1994. **43**(8): p. 772-780.


92. Healy, K.E., A. Reznia, and R.A. Stile, *Designing biomaterials to direct biological responses*, in *Bioartificial Organs II: Technology, Medicine, and Materials*, D. Hunkeler, et al., Editors. 1999, New York Acad Sciences: New York. p. 24-35.

93. He, Y. and Y. Inoue, *Novel FTIR method for determining the crystallinity of poly(epsilon-caprolactone)*. Polymer International, 2000. **49**(6): p. 623-626.

94. Blomqvist, J., B. Mannfors, and L.O. Pietila, *Amorphous cell studies of polyglycolic, poly(L-lactic), poly(L,D-lactic) and poly(glycolic/L-lactic) acids*. Polymer, 2002. **43**(17): p. 4571-4583.

95. Reeve, M.S., et al., *POLYLACTIDE STEREOCHEMISTRY - EFFECT ON ENZYMATIC DEGRADABILITY*. Macromolecules, 1994. **27**(3): p. 825-831.





96. Jenkins, M.J. and K.L. Harrison, *The effect of molecular weight on the crystallization kinetics of polycaprolactone*. *Polymers for Advanced Technologies*, 2006. **17**(6): p. 474-478.

97. Gilding, D.K. and A.M. Reed, *BIODEGRADABLE POLYMERS FOR USE IN SURGERY - POLYGLYCOLIC-POLY(ACTIC ACID) HOMOPOLYMERS AND COPOLYMERS*. *J. Polymer*, 1979. **20**(12): p. 1459-1464.

This volume is the property of the University of Oklahoma, but the literary rights of the author are a separate property and must be respected. Passages must not be copied or closely paraphrased without the previous written consent of the author. If the reader obtains any assistance from this volume, he or she must give proper credit in his own work.

I grant the University of Oklahoma Libraries permission to make a copy of my thesis upon the request of individuals or libraries. This permission is granted with the understanding that a copy will be provided for research purposes only, and that requestors will be informed of these restrictions.

NAME

DATE

[REDACTED]  
[REDACTED]

A library which borrows this thesis for use by its patrons is expected to secure the signature of each user.

This thesis by JIMMY DAVID MURRAY has been used by the following persons, whose signatures attest their acceptance of the above restrictions.

---

NAME AND ADDRESS

DATE